BIOCHEMICAL PHARMACOLOGY 73 (2007) 417–426

available at www.sciencedirect.com

ScienceDirect

journal homepage: www.elsevier.com/locate/biochempharm

Chain length dependence of the interactions of bisquaternary ligands with the *Torpedo* nicotinic acetylcholine receptor

Chris R.J. Carter [a], *Liren Cao* [b,1], *Hideki Kawai* [c,2], *Peter A. Smith* [a,b], *William F. Dryden* [a,b], *Michael A. Raftery* [d], *Susan M.J. Dunn* [a,b,*]

[a] *Department of Pharmacology, University of Alberta, Edmonton, Alberta, Canada T6G 2H7*
[b] *Centre for Neuroscience, University of Alberta, Edmonton, Alberta, Canada T6G 2S2*
[c] *Department of Pharmacology, University of Minnesota, Minneapolis, MN 55455-0217, USA*
[d] *Department of Biochemistry, Molecular Biology and Biophysics, University of Minnesota, Minneapolis, MN 55455, USA*

ARTICLE INFO

Article history:
Received 18 July 2006
Accepted 16 October 2006

Keywords:
Torpedo nicotinic acetylcholine receptor
Bisquaternary agonists
Suberyldicholine
Xenopus oocyte expression
Ligand-gated ion channels

ABSTRACT

The interactions of a series of bisholine esters $[(CH_3)_3N^+CH_2CH_2OCO–(CH_2)_n–COOCH_2CH_2N^+(CH_3)_3]$ with the *Torpedo* nicotinic acetylcholine receptor have been investigated. In equilibrium binding studies, [^{3}H]-suberyldicholine ($n = 6$) binds to an equivalent number of sites as [^{3}H]-acetylcholine and with similar affinity ($K_D \sim 15$ nM). In competition studies, all bischoline esters examined displaced both radioligands in an apparently simple competitive manner. Estimated dissociation constants (K_I) showed clear chain length dependence. Short chain molecules ($n \leq 2$) were of lower affinity (K_I's of 150–300 nM), whereas longer ligands ($n > 6$) had high affinity similar to suberyldicholine. Functional responses were measured by either rapid flux techniques using *Torpedo* membrane vesicles or voltage-clamp analyses of recombinant receptors expressed in *Xenopus* oocytes. Both approaches revealed that suberyldicholine (EC50 $\sim$ 3.4 μM) is 14–25-fold more potent than acetylcholine. However, suberyldicholine elicited only about 45% of the maximum response of the natural ligand, i.e., it is a partial agonist. The potency of this bischoline series increased with chain length. Whereas the shorter ligands ($n \leq 3$) displayed potencies similar to acetylcholine, longer ligands ($n \geq 4$) had similar (or higher) potency to suberyldicholine. Ligand efficacy had an approximately bell-shaped dependence on chain length and compounds where $n \leq 3$ and ≥ 8 were very poor partial agonists. Based on estimates of interonium distances, we suggest that bisquaternary ligands can interact with multiple binding sites on the nAChR and, depending on the conformational state of the receptor, these sites are 15–20 Å apart.

* *Corresponding author at*: Department of Pharmacology, University of Alberta, Edmonton, Alberta, Canada T6G 2H7. Tel.: +1 780 492 3414; fax: +1 780 492 4325.
E-mail address: susan.dunn@ualberta.ca (Susan M.J. Dunn).
[1] Present address: MedCell Biotech Co., Room 206, Ke-Mao-Yi-Lou, No. 12 Zhongguancun Nandajie, Haidian District, Beijing 10081, China.
[2] Present address: Department of Neurobiology and Behavior, University of California, Irvine, CA 92697, USA.
0006-2952/$ – see front matter
doi:10.1016/j.bcp.2006.10.011

1. Introduction

The peripheral (muscle-type) nicotinic acetylcholine receptor (nAChR) is the prototype of the "cys-loop" family of ligand-gated ion channels (LGICs) that includes the neuronal nAChRs in addition to the 5-hydroxytryptamine type 3 ($5HT_3$), γ-amino-butyric acid type A ($GABA_A$) and glycine receptors. The best characterized member of the family is the nAChR from *Torpedo* electric organ. This large, complex transmembrane protein is a pentamer of homologous subunits ($\alpha_2\beta\gamma\delta$) that assemble pseudosymmetrically to form a central cation-selective ion channel [1–3]. There is considerable biochemical and mutational evidence to demonstrate that a high affinity binding site for agonists and competitive antagonists lies at each of the α–γ and α–δ subunits interfaces where they are formed by at least six (A–F) non-contiguous "loops" of amino acids [4–6]. The α-subunit is suggested to contribute loops A–C while the neighbouring subunits contribute loops D–F. The non-equivalence of the interfaces confer distinct recognition properties for at least some agonists [7] and competitive antagonists [8–11].

The requirements for neurotransmitter activation of members of this LGIC family appear to be less rigorous than those of enzyme–substrate interactions that have precise stereochemical requirements for catalysis. Although the neurotransmitter binding sites within the nAChR display selectivity, they are also sufficiently spacious and flexible to accommodate ligands with a diverse range of chemical structures. Ligands that interact with these sites show a spectrum of activities ranging from antagonists to full agonists. Well-characterised ligands include the large antagonist α-neurotoxins, complex alkaloids such as D-tubocurarine and small monoquaternary agonists, such as acetylcholine (ACh) and phenyltrimethylammonium. While a great deal of evidence on the location of these sites has accumulated over the last several decades, direct evidence remains lacking, since the nAChR (like the other members of this LGIC family) has thus far proved intransigent to crystallization. However, the reported crystal structure of a snail acetylcholine binding protein (AChBP) that is homologous to the extracellular domains of the LGIC family [12] has proved to be a useful template on which to model binding domains. Since the structure of the AChBP strongly supports earlier notions of binding site architecture and the location of binding "loops" at the subunit–subunit interfaces, this has rejuvenated interest in structure–function relationships of the LGICs.

In this study, we focus on the binding and functional properties of the bischoline ester series exemplified by

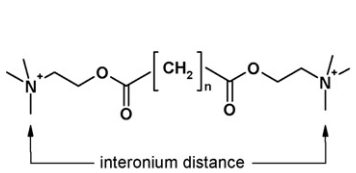

Bis-choline	n	distance (Å)
oxalyl	0	11.2
malonyl	1	12.2
succinyl	2	13.3
glutaryl	3	14.7
adipyl	4	16.0
pimelyl	5	17.3
suberyl	6	18.7
azelyl	7	20.0
sebacyl	8	21.3
dodecanyl	10	24.0

Fig. 1 – The structure of the bischoline analogues. The interonium distances of the extended ligand conformations were estimated using WebLab Viewer Lite (Accelrys, San Diego, CA).

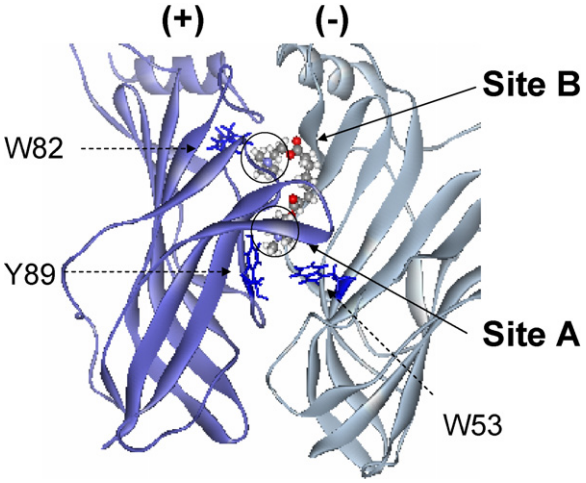

Fig. 2 – A model illustrating how SbCh may crosslink two subsites in the nAChR. The figure shows a side view of a subunit–subunit interface of the AChBP [12], a homologue of the extracellular domain of the LGIC family. SbCh is depicted as binding to the well characterized high affinity site (site A) which includes residues Y89, lying in loop A of the principal (+)-subunit and W53 lying in loop D of the subordinate (−)-subunit [4–11]. The conformation of SbCh shown is one of many that this large, flexible ligand can adopt. Although the location of site B remains speculative, here we depict this site as including W82 of the principal subunit. This residue lies in the homologous position to W86 in the *Torpedo* nAChR α-subunit, a residue that we have recently shown to be important for activation of the *Torpedo* receptor by SbCh, but not by ACh [17].

suberyldicholine (SbCh; Fig. 1). The unusual effects of bisquaternary cholinergic antagonists acting at the neuromuscular junction and the strong correlation between the interonium distance of the compound and its ability to block neuromuscular transmission has long been recognized (see [13]). As discussed in an early treatise by Michaelson and Zeimal [14], results obtained with bisquaternary ligands have given considerable insights into the nature of cholinergic binding sites and provided early evidence to suggest that multiple subsites may exist within each neurotransmitter binding domain. We previously reported differences in the binding of SbCh and ACh to the *Torpedo* nAChR [15,16]. Based on studies of the kinetics of dissociation and association of these ligands, a model was proposed in which each of the two high affinity sites on the nAChR is composed of two subsites (sites A and B; see Fig. 2) that are allosterically coupled. It was suggested that, although the two subsites are mutually exclusive for ACh under equilibrium conditions, the large bisquaternary SbCh may be able to physically bridge these subsites. A preliminary study of the kinetics of association of this series of bischoline esters placed physical constraints on the potential distance between these sites [16]. Ligands of the size of pimelyldicholine (one methylene group shorter than SbCh) and longer displayed SbCh-like kinetics, whereas shorter bisquaternary ligands displayed ACh-like characteristics. The interonium distance of the extended conformation of pimelyldicholine is approximately

17.3 Å (Fig. 1) suggesting that, under the conditions of these experiments, the putative subsites may be separated by approximately this distance (see Fig. 2).

In the present report, the interactions of bischoline esters with the *Torpedo* nAChR have been examined using both native membrane-bound receptors and recombinant *Torpedo* nAChRs expressed in *Xenopus* oocytes. It is shown that the apparent affinities of these ligands, measured in both binding and functional studies, are correlated with their interonium distance. However, the maximum responses induced by the bischoline esters are significantly less than the maximum response elicited by ACh, i.e., all bisquaternary ligands examined are partial agonists. The results shed further light on multiple binding domains within the nAChR structure and how their occupancy may be related to receptor function.

2. Materials and methods

2.1. Materials

ACh, SbCh and succinyldicholine were from Sigma Chemical Company. The other bischoline esters were synthesized from their corresponding acid chlorides (obtained from Aldrich Chemical Company) using established procedures [16]. [^{3}H]ACh and [^{125}I]α-bungarotoxin (α-BTx) were from DuPont Canada (Mississauga, ON). [^{3}H]SbCh was synthesized as previously described [15]. 8-Amino-1,3,6-naphthalene trisulfonic acid (ANTS) was from either Chem Service Inc. (West Chester, PA) or Molecular Probes Inc. (Eugene, OR) and 1,3,6,8-pyrenetetrasulfonic acid (PTSA) was from Molecular Probes. Restriction enzymes and cRNA transcript preparation materials were from Invitrogen (Burlington, ON), New England Biolabs (Pickering, ON) or Promega (Madison, WI). The γ-subunit cDNA clone (in the SP64-based plasmid, pMXT) of the *Torpedo* nAChR was kindly provided by Dr. J.B. Cohen (Harvard Medical School, Boston, MA), while the δ-subunit (in the SP65 plasmid), as well as the α- and β-subunits (in the SP64 plasmid) cDNA clones were generous gifts from Dr. H.A. Lester (California Institute of Technology, Pasadena, CA).

2.2. Preparation of nAChR-enriched membrane fragments

Membrane fragments enriched in nAChR were prepared from frozen *Torpedo californica* electric organ (Pacific Biomarine, Venice, CA or Aquatic Research Consultants, San Pedro, CA) as described previously [18]. Membrane suspensions were stored at −85 °C before use. Protein concentrations were determined using the BioRad (Mississauga, ON) assay and the concentration of receptor sites for [^{125}I]α-BTx was measured by the DEAE-disc assay [19]. As indicated in the text, for some experiments, nAChR-enriched membranes were first alkali-extracted at pH 11 to remove peripheral membrane proteins [20,21].

2.3. Equilibrium binding of [^{3}H]Ach and [^{3}H]SbCh to membrane-bound nAChR

Measurements of [^{3}H]ACh and [^{3}H]SbCh binding were carried out using centrifugation assays [15]. Prior to binding assays, acetylcholinesterase activity in concentrated non-alkali extracted membrane fragments (approximately 5 mg protein/ml) was inhibited by the addition of 1/200 volume of a 0.3 M stock solution of diethyl-*p*-nitrophenyl phosphate (DNPP, Sigma) prepared in isopropanol. After 3 min at room temperature, the membranes were diluted by about 10-fold in *Torpedo* Ringer's solution (20 mM Hepes-Na^+, 250 mM NaCl, 5 mM KCl, 4 mM $CaCl_2$, 2 mM $MgCl_2$, 0.02% NaN_3, pH 7.4) and stored on ice until use. Aliquots of DNPP-treated membranes were added to various concentrations of [^{3}H]ACh or [^{3}H]SbCh in *Torpedo* Ringer's solution to give a final protein concentration of 0.1 mg/ml in a final volume of 0.5 ml. After incubation for 45 min at room temperature, duplicate 50 μl aliquots were removed for estimation of the total added radioligand concentration. The remaining samples were centrifuged at 12,000 × *g* for 15 min at 4 °C, after which duplicate 50 μl aliquots of the supernatant were removed for determination of the free radioligand concentration. The amount of bound radioligand was calculated by subtracting free from total ligand concentration. Non-specific binding was determined from parallel measurements of binding in the presence of excess unlabeled ligand (1 mM ACh or 1 mM SbCh).

2.4. Competition assays

Displacement experiments were carried out using a centrifugation procedure similar to that described above. Aliquots of DNPP-treated *Torpedo* membranes (final concentration of 0.1 mg/ml) were incubated with either 0.2 μM [^{3}H]ACh or [^{3}H]SbCh and increasing concentrations of unlabelled ligand (0–1 mM) for 30 min at room temperature before quantification of the concentrations of bound and free radioligand as above.

2.5. Thallium (1) flux assays

Stopped-flow measurements of agonist-induced Tl^+ flux using alkali-extracted *Torpedo* membrane preparations were carried out using a fluorescence assay modified from that of Moore and Raftery [22] after loading of the membrane vesicles with either of the membrane-impermeant fluorescent probes, ANTS or PTSA [23]. The kinetics of Tl^+ influx were measured using an Applied Photophysics (Leatherhead, UK) SF.17 MV Microvolume instrument and appropriate wavelengths for each dye. Briefly, a suspension of fluorophore-loaded vesicles (in 10 mM nitrilotriethanol, 35 mM $NaNO_3$, pH 7.4) was mixed rapidly with an equal volume of a solution of agonist (in 10 mM nitrilotriethanol, 35 mM $TlNO_3$, pH 7.4) at 25 °C and the kinetics of the fluorescence quench resulting from Tl^+ influx were monitored using an Archimedes computer and Applied Photophysics software.

2.6. In vitro transcription

Plasmid cDNAs encoding the *Torpedo* nAChR subunits were linearized by digestion with *Xba*I (γ- and δ-subunits), *Eco*RI (α-subunit) or *Fsp*I (β-subunit). *In vitro* transcription of cRNA was performed using methods previously described [24]. Briefly, the linearized cDNA templates (5 μg) were transcribed *in vitro*

by SP6 RNA polymerase (Promega) in the presence of RNA capping analogue (New England Biolabs) and ribonucleotide triphosphates (NTP mix, Invitrogen). RNA transcripts were then extracted using a 25:24:1 (v/v/v) phenol:chloroform:isoamyl alcohol mixture. Final cRNA pellets were resuspended in diethylpyrocarbonate-treated water to a final concentration of 1 μg/μl and aliquots were stored at −80 °C until use.

2.7. Expression in Xenopus oocytes and electrophysiology

Isolated, follicle-free oocytes from *Xenopus laevis* were microinjected with a total of 50 ng of subunit cRNAs in the ratio of 2α:1β:1γ:1δ. Oocytes were incubated in ND96 buffer (5 mM Hepes, 96 mM NaCl, 1.8 mM $CaCl_2$, 2 mM KCl, 1 mM $MgCl_2$, pH 7.6) supplemented with 50 μg/ml gentamicin at 14 °C for at least 48 h prior to recording. Currents elicited by bath application of agonist were measured using standard two-electrode voltage clamp techniques and a GeneClamp500 amplifier (Axon Instruments, Foster City, CA) with a holding potential of −60 mV. Electrodes were filled with 3 M KCl and only electrodes with resistances of 0.5–3.0 MΩ were used. The recording chamber was continuously perfused (at a rate of ~5 ml/min) with low calcium ND96 buffer (as above but with the $CaCl_2$ concentration reduced to 0.1 mM) supplemented with 1 μM atropine. Atropine was included in the perfusion buffer to block the effects of endogenous muscarinic receptors present on the surface of the oocytes [25] and the Ca^{2+} concentration was reduced to decrease the rate of receptor desensitization [26]. Agonist–evoked responses were measured by applying drug (via the perfusion system) for 10–20 s unless otherwise indicated. Drugs were washed out for 12 min between applications to ensure complete recovery from desensitization.

2.8. Data analysis

Binding data were analysed using GraphPad Prism (San Diego, CA) software. Saturation binding data (after correction for non-specific binding) were fit by a simple binding isotherm:

$$[\mathrm{RL}] = \frac{[\mathrm{R_0}][\mathrm{L}]}{K_\mathrm{D} + [\mathrm{L}]}$$

where [RL], [R_0] and [L] are the concentrations of occupied receptor, available receptor sites and free radioligand concentration, respectively.

Displacement of radiolabelled ligand by unlabelled ligands were fit by a simple competition curve:

$$[\mathrm{RL}] = [\mathrm{RL}]_\mathrm{min} + \frac{[\mathrm{RL}]_\mathrm{max} - [\mathrm{RL}]_\mathrm{min}}{1 + 10^{(\log[\mathrm{X}] - \log \mathrm{IC_{50}})}}$$

where [RL] is bound radioligand, $[RL]_{min}$ and $[RL]_{max}$ are the minimum and maximum amount of bound radioligand measured, [X] the total concentration of competing ligand and IC_{50} is the concentration of the unlabelled ligand that causes 50% displacement.

Apparent K_I values were calculated using the Cheng–Prusoff equation [27]:

$$K_\mathrm{I} = \frac{\mathrm{IC_{50}}}{1 + [\mathrm{L}]/K_\mathrm{D}}$$

where K_D is the equilibrium dissociation constant for the radioligand used in the assay and other parameters are as defined above.

The kinetic traces for thallium (1) flux were fit using Applied Photophysics software and a modified Stern–Volmer equation [22]:

$$F(t) = \frac{A_1}{1 + KT_\infty(1 - \mathrm{e}^{-k_\mathrm{app}t})} + k_0 t + A_0$$

where $F(t)$ is the fluorescence intensity at time t, A_1 the amplitude of the specific agonist-induced fluorescence quench, K the Stern–Volmer constant for quenching of the fluorophore by Tl^+ (96 M^{-1} for ANTS or 201 M^{-1} for PTSA), T_∞ the final concentration of Tl^+, k_{app} the apparent rate constant of Tl^+ flux, k_0 the rate of Tl^+ leak through the membrane and A_0 is the baseline fluorescence intensity.

The concentration dependence of the rate of agonist-induced Tl^+ flux was fit using GraphPad software and the sigmoidal equation:

$$k_\mathrm{app} = k_\mathrm{min} + \frac{k_\mathrm{max} - k_\mathrm{min}}{1 + 10^{(\log[\mathrm{X}] - \log \mathrm{EC_{50}})^{n_\mathrm{H}}}}$$

where k_{app} is the apparent rate constant at each concentration of ligand, [X], k_{min} and k_{max} are the minimum and maximum rates, respectively, and n_H is the apparent Hill coefficient.

The peak amplitudes of agonist-induced current responses of recombinant receptors expressed in *Xenopus* oocytes were analyzed using Axoscope 8 software. Concentration-effect curves were analyzed using GraphPad Prism software and the following equation:

$$I = \frac{I_\mathrm{max}[\mathrm{L}]^{n_\mathrm{H}}}{\mathrm{EC_{50}} + [\mathrm{L}]^{n_\mathrm{H}}}$$

where I is the measured agonist–evoked current, [L] the agonist concentration, EC_{50} the agonist concentration that evokes half the maximal current (I_{max}) and n_H is the apparent Hill coefficient.

3. Results

3.1. Binding of [^{3}H]ACh and [^{3}H]SbCh to Torpedo membrane preparations

In agreement with previous results in which alkali-extracted *Torpedo* membranes were used [15], the binding of both radioligands was to an apparently homogeneous population of high affinity sites (Fig. 3A). In replicate experiments (5–8 determinations), the estimated dissociation constant (K_Ds) for [^{3}H]SbCh and [^{3}H]ACh binding were 14.9 ± 2.5 and 11.4 ± 1.9 nM, respectively, and binding was to an equivalent number of sites (approximately 0.4 nmol/mg protein). Thus, these ligands display very similar binding characteristics under equilibrium conditions.

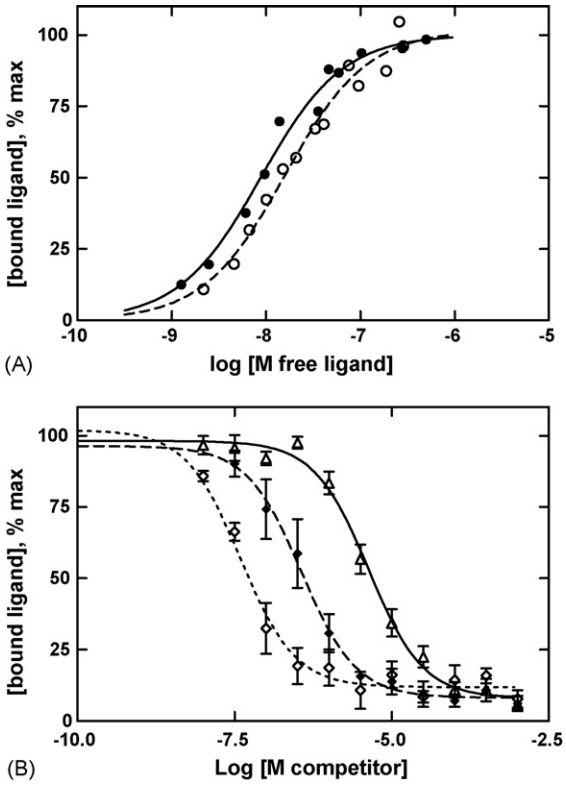

Fig. 3 – (A) Representative data for the equilibrium binding of [^{3}H]ACh (●) and [^{3}H]SbCh (○) to nAChR-enriched membrane fractions. The lines represent the best-fit curves to a simple non-cooperative binding model with estimated K_D values of 8.8 nM for ACh and 15.9 nM for SbCh. In replicate experiments, the binding of each ligand was to an approximately equal number of sites with similar affinities for the two agonists (see text for parameters). (B) Representative data for displacement of [^{3}H]ACh by azelyl (◇), malonyl (△) and adipyldicholine (◆). All bischolines appear to displace the radioligand in a simple competitive manner and best-fit parameters for these and other bischolines in the series are shown in Table 1.

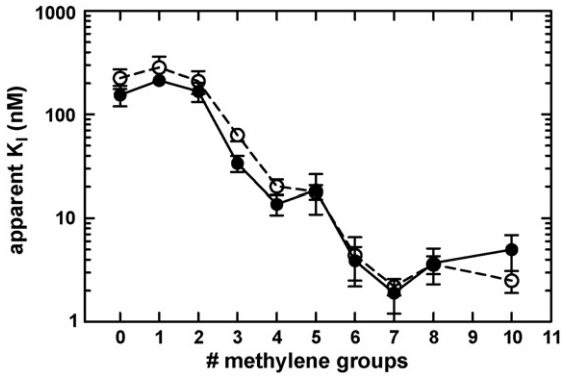

Fig. 4 – The relative affinities of bischoline analogues for the membrane-bound *Torpedo* nAChR measured in competitive binding assays. The concentration dependencies for displacement of [^{3}H]ACh (●) or [^{3}H]SbCh (○) by bischoline ligands were used to estimate K_I values. The data represent the mean ± S.E.M. of 3–8 independent experiments and the best fit parameters from curve fitting are summarized in Table 1.

3.2. *Affinities of the bischoline esters measured in competition assays*

In displacement studies, ACh and SbCh appear to interact with the membrane-bound *Torpedo* receptor in a simple competitive manner. Unlabelled SbCh displaced all bound [^{3}H]ACh with an estimated K_I of 3.9 ± 1.4 nM (n = 3) and unlabelled ACh caused complete displacement of [^{3}H]SbCh with a K_I of 17.1 ± 1.0 nM (n = 3). These results are in reasonable agreement with the direct binding assays shown in Fig. 3A. Similar competition assays have been carried out to study the displacement of either [^{3}H]ACh or [^{3}H]SbCh by the bischoline esters shown in Fig. 1. Representative displacement curves are shown in Fig. 3B. In no case was there any evidence for binding site heterogeneity and a simple competitive equation adequately described all of the displacement data. Fig. 4 illustrates the estimated K_I values for all of the ligands as a function of their chain length, i.e., number of methylene groups (n).

Table 1 – Summary of binding and functional data for the effects of bischoline esters using nAChR in native *Torpedo* membrane vesicles or recombinant *Torpedo* nAChRs expressed in *Xenopus* oocytes

Bischoline ester (n)	*Torpedo* membranes			*Xenopus* oocytes		
	[^{3}H]ACh displacement, K_I (nM)	[^{3}H]SbCh displacement, K_I (nM)	Tl^+ flux, EC_{50} (μM)	Current, EC_{50} (μM)	n_H	Efficacy, I_{max}/I_{max}ACh (%)
Oxalyl (0)	154 ± 34	225 ± 48	79.3 ± 9.9	>1000	–	0.8 ± 0.6
Malonyl (1)	213 ± 23	284 ± 78	85.9 ± 12.6	270 ± 25	2.28 ± 0.18	4.8 ± 0.5
Succinyl (2)	167 ± 35	209 ± 53	61.1 ± 8.4	–	–	–
Glutaryl (3)	33.7 ± 5.9	63.2 ± 8.2	34.2 ± 2.1	34.3 ± 0.3	1.36 ± 0.09	12.6 ± 1.9
Adipyl (4)	13.7 ± 1.4	20.2 ± 3.4	6.8 ± 1.7	5.7 ± 1.0	1.28 ± 0.13	73.6 ± 7.5
Pimelyl (5)	18.7 ± 7.8	17.9 ± 2.8	6.4 ± 1.4	10.8 ± 1.3	1.16 ± 0.07	36.6 ± 9.4
Suberyl (6)	3.9 ± 1.4	4.4 ± 2.2	3.4 ± 1.0	3.42 ± 0.35	1.47 ± 0.26	45.3 ± 1.9
Azelyl (7)	1.9 ± 0.7	2.2 ± 0.4	n.d.	1.03 ± 0.06	1.07 ± 0.08	42.6 ± 11.3
Sebacyl (8)	5.0 ± 1.9	3.6 ± 0.7	n.d.	0.28 ± 0.05	2.91 ± 0.27	5.4 ± 0.8

n.d.: not determined; –: parameters could not be obtained due to the low amplitude of the current.

Parameters obtained from data fitting are summarized in Table 1. These data show a clear chain length dependence on equilibrium binding affinity. The short chain derivatives (oxalyl, malonyl and succinyl; where $n = 0$, 1 and 2, respectively; see Fig. 1) display relatively low affinity (with K_I's about 10-fold higher than the K_D for ACh binding), but larger ligands ($n \geq 6$), i.e., suberyldicholine and longer, were of higher affinity comparable to that of ACh. The intermediate length members of the series displayed intermediate affinity.

3.3. *The effects of ACh and SbCh on activation of Torpedo nAChR*

Fig. 5A shows representative concentration-effect curves for agonist-mediated flux responses of the native membrane-bound *Torpedo* receptor measured using stopped-flow fluorescence techniques. Results from at least six replicate experiments gave EC_{50} values of 3.4 ± 1.0 and 83 ± 16 μM for SbCh and ACh, respectively, showing that SbCh is approximately 24-fold more potent than ACh. However, SbCh is only a partial agonist of the *Torpedo* nAChR. In Tl^+ flux assays, SbCh consistently elicited only about 30% of the maximum rate of the response induced by ACh. Due to inherent difficulties in accurately determining the maximum flux rates using this approach, this provides only an approximation of the relative efficacies of these agonists (see below). In the recombinant receptor expressed in *Xenopus* oocytes (Fig. 5B), the potencies of SbCh and ACh were within a factor of two of the native receptor with measured EC_{50} values of 3.4 ± 0.4 and 46 ± 9 μM, respectively. SbCh is also a partial agonist in this system and, as shown in the inset in Fig. 5B, the maximum current that this ligand elicits is only about 46% of the maximum ACh response (see also Fig. 6B).

3.4. *Potency of bischoline esters*

The functional responses of this series of bischoline compounds were measured using both receptor-enriched membranes from *Torpedo* electric organ (using the Tl^+ flux method) and the recombinant receptor expressed in *Xenopus* oocytes (using two-electrode voltage clamp techniques). The measured EC_{50} values for the functional responses are shown as a function of chain length in Fig. 6A (see also Table 1). As was seen in the binding assays (Fig. 4), there is a clear chain length dependence with the potency of the ligand becoming greater with increasing number of methylene groups. In these experiments, it should be noted that accurate analyses of the activation of the *Torpedo* receptor by the shortest and longest members of this series is complicated by the low amplitude of responses induced by these ligands (see below).

In general, the results obtained using the two systems (*Torpedo* membranes versus recombinant receptors) were in good agreement suggesting that the oocyte expression system faithfully reproduces the properties of the native nAChR. There were, however, some unexpected results. Using *Torpedo* membranes, the binding of the shortest bischoline ester, oxalyldicholine ($n = 0$) was robust, as revealed by its ability to displace all [^{3}H]ACh and [^{3}H]SbCh from its binding sites. In Tl^+ flux assays, it elicited a response that was close to that of carbamylcholine (data not shown) allowing estimates of its

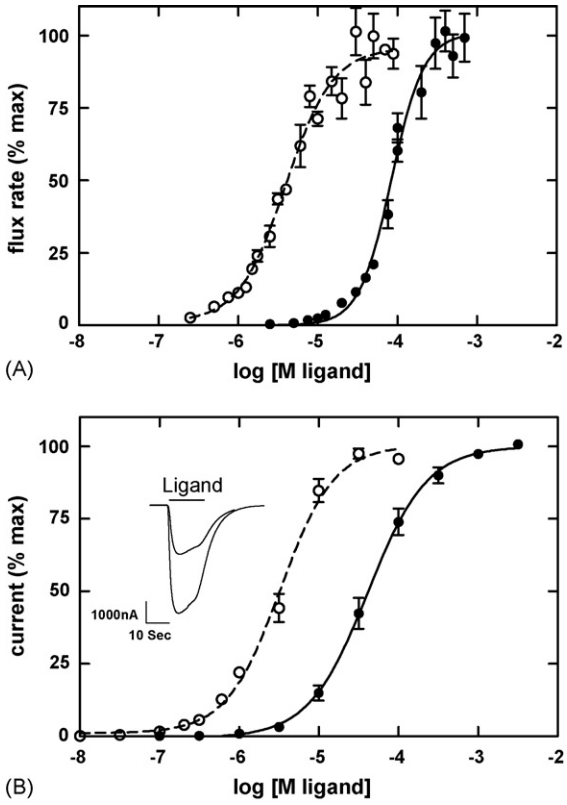

Fig. 5 – Functional responses mediated by ACh and SbCh. (A) Representative concentration-effect curves for activation of the native *Torpedo* nAChR by ACh (●) and SbCh (○) measured in Tl^+ flux assays. In each case, the measured rate was normalised to the maximum rate of flux evoked by the same ligand. Data fitting as described in the text gave an EC_{50} value of 3.9 μM and n_H of 1.47 for SbCh. Corresponding values for ACh were 84.8 μM and 2.07, respectively. In the case of ACh, the flux rates at high concentrations exceeded the time resolution of the stopped-flow technique and this required partial inactivation of the receptor by pre-treatment with 1–3 μM histrionicotoxin. Flux rates under these conditions were normalized using the factor by which histrionicotoxin slowed the flux rate at 30 μM ACh (see [22], for details). (B) Concentration-effect curves for activation of the recombinant nAChR by ACh (●) and SbCh (○). The data shown are normalized to the measured I_{max} value for each agonist and represent the mean ± S.E.M. from at least three independent experiments. Curve fitting analysis as described in the text gave EC_{50} values of 3.42 ± 0.35 μM for SbCh and 46.5 ± 9.4 μM for ACh (Table 1). The inset illustrates the partial agonist activity of SbCh in the recombinant receptor and show representative traces for activation by E_{max} concentrations of ACh (1 mM, lower trace) and SbCh (100 μM, upper trace). In three independent experiments in which full concentration-effect curves were analyzed, the maximum current evoked by SbCh reached only 45.2% of that elicited by ACh (see also Fig. 6B).

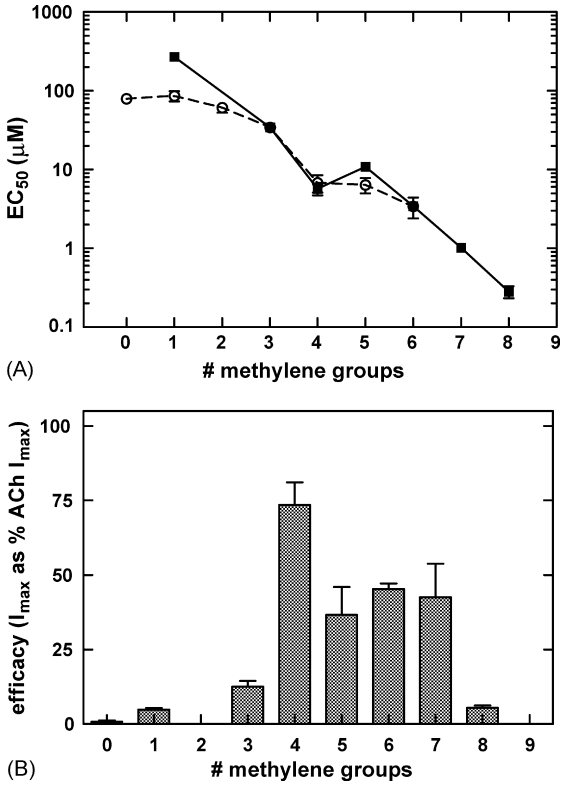

Fig. 6 – Potencies and efficacies of the bischoline analogues measured in functional studies. (A) Apparent EC_{50} values obtained from voltage-clamp analysis of recombinant receptors expressed in *Xenopus* oocytes (■) are in good agreement with estimates obtained from fluorescence assays of Tl^+ flux responses of native nAChRs in *Torpedo* membrane vesicles (○). (B) Relative efficacies of bischoline-induced current responses of recombinant *Torpedo* nAChRs. The data represent the mean ± S.E.M. of the maximum response for each ligand (obtained from full-concentration-effect curves) compared to the maximum response elicited by a saturating concentration of ACh.

EC_{50} for channel activation (see Table 1). In contrast, oxalyldicholine elicited barely detectable currents in the recombinant receptor. Succinylcholine ($n = 2$) had very low efficacy in both systems. In the recombinant receptor, the induced currents were too small to be analysed accurately, but a small Tl^+ flux response (less than 5% of that induced by carbamylcholine) has allowed approximation of the activation parameters for this ligand (Table 1). Long chain analogues ($n = 9$ or 10) induced such small responses that no estimates of their activation parameters could be obtained.

3.5. *Efficacies of the bischoline ligands*

Determination of efficacy, i.e., the magnitude of the response that can be elicited by a particular ligand, requires that the maximum response to a full agonist can be measured reliably. In this respect, the Tl^+ flux assay suffers from the disadvantage that the maximum rates of flux must be measured. Although ACh is likely to be a full agonist of the *Torpedo* nAChR, the rate of its maximum Tl^+ flux response may exceed the resolution of stopped-flow instruments (see [22]; also Fig. 5A) and depends also on both membrane vesicle integrity and the number of receptors per vesicle. We have, therefore, used the oocyte expression system to provide more reliable estimates of the efficacies of different members of the bischoline series. The advantage of this system is that the maximum responses to multiple ligands can be measured in the same oocyte thus obviating problems arising from variations in levels of receptor expression. The results in Fig. 6B demonstrate that none of the bischoline esters were more efficacious than ACh. Furthermore, there is clear trend in the chain-length dependency of the response, i.e., bischoline derivates in which $n \leq 3$ are poor partial agonists as are those in which $n > 7$. Qualitatively similar results (except in the case of oxalyldicholine as noted above) have been observed in Tl^+ flux assays.

4. Discussion

There is a wealth of experimental data to suggest that, under equilibrium conditions, the *Torpedo* nAChR carries two high affinity sites for agonists/competitive antagonists and that these sites lie at the interfaces between the α–γ and α–δ subunits [4–6]. However, an inevitable complication in studying structure–function relationships of the nAChR is that the receptor, like most of the ligands with which it interacts, is inherently flexible. Since, both the protein and ligand can adapt to changes in its environment, the receptor–agonist complex can adopt multiple conformations, some of which may exist only transiently in the pathways leading to receptor activation and/or desensitization.

In early whole animal experiments of the neuromuscular blocking activities of a series of polymethylenebis(trimethylammonium) compounds, two maxima were observed for compounds having a bisonium bridge of 10 or 16–18 methylene groups, whereas in the corresponding bis(triethylammonium) series, only the second maximum was observed (see [13,14]). Direct studies of the interaction of a series of 1,*n*-bis(3-aminopyridinio)-alkane fluorescent derivatives with the *Torpedo* nAChR later revealed that compounds with 12–16 methylene groups were of significantly higher affinity than their shorter or longer analogues [28]. In their extended conformations, the high affinity compounds have estimated interonium distances of 16.8–21.4 Å, approximating the size of pimelyl- ($n = 5$) to sebacyldicholine ($n = 8$) used in the present study (Fig. 1). This clear chain length dependence suggests that separate binding domains contribute to the recognition of the two quaternary groups of these ligands.

Other studies using photoisomerizable bisquaternary ligands [29] have provided insights as to the involvement of these putative subsites in receptor activation. In the *Electrophorus* nAChR, *cis*-3,3′-bis[α-(trimethylammonium)methyl]azobenzene dibromide is an antagonist, whereas the *trans*-isomer is a potent agonist [30,31]. These isomers cannot occupy the same physical space within the receptor binding site(s). Using an alkylating monoquaternary analogue (QBr), which was likely to have been tethered to residues C192/193 of the α-subunit [32], it was shown that receptor activation occurred only when the ligand was photolyzed to its

trans-conformation. In the *trans*-isomer, the quaternary ammonium group lies approximately 14 Å away from the tethering site, suggesting that a site involved in activation lies approximately this distance from Cys192/193. Unlike the eel receptor, in the *Torpedo* nAChR, both Bis Q isomers act as antagonists ([30]; also unpublished results) showing that these receptor subtypes discriminate in their responses to different ligands. One possible explanation is that there are (perhaps subtle) differences in the distance between the putative subsites.

The present study has investigated the interaction of bischoline esters with the *Torpedo* nAChR under two sets of conditions, i.e., rapid ion conductance responses measured soon after exposure of the resting (activatable) receptor to ligand, and radiolabelled binding studies carried out under equilibrium conditions. The equilibrium binding of [^{3}H]ACh and [^{3}H]SbCh to the membrane-bound *Torpedo* nAChR suggests that each ligand binds to an apparently homogeneous population of sites with similarly high affinity. Displacement of these radioligands by all of the bischoline ester compounds examined was consistent with a simple competitive model. Thus, these equilibrium-binding studies did not reveal the complexity of receptor–ligand interactions that we observed previously in kinetic studies [15,16]. After saturation of all of the high affinity sites on the *Torpedo* receptor with radiolabelled ACh or SbCh, we showed that the rate of dissociation of [^{3}H]ACh (but not that of [^{3}H]SbCh) was significantly accelerated upon dilution into buffer containing micromolar concentrations of unlabelled cholinergic ligands. Detailed examination of this phenomenon led us to suggest that each of the high affinity sites (designated as site A) is associated with a secondary subsite (site B) to which it is allosterically coupled. We suggested that these two subsites may be ''crosslinked'' by the large bisquatemary ligand, SbCh. In fluorescence studies of agonist association, evidence for transient occupancy of two subsites for ACh, but not for SbCh was obtained [16]. As noted in the Introduction, the shortest ligand to display SbCh-like association kinetics was pimelyldicholine ($n = 5$). In the present study, adipyldicholine ($n = 4$) displayed similar equilibrium binding properties to pimelyldicholine (Table 1). These results can be rationalized by considering the differences in the timescales of the two sets of experiments. The fluorescence studies monitor initial binding events, whereas radioligand binding studies reflect the equilibrium state. As noted above, the receptor and/or ligand may adopt different conformations during the approach to equilibrium. Thus, the distance between the putative subsites is unlikely to be identical in each conformation of the complex.

Here, we have extended our studies of the bischoline series to include detailed characterization of functional responses. Overall, the potencies of these ligands follow a similar trend to their equilibrium binding affinities. Although the shorter bischolines ($n = 0$–2) bound with approximately 10-fold lower affinity, their EC_{50} values were similar to those of ACh measured in both Tl^+ flux studies ($EC_{50} \sim 80$ μM) and in *Xenopus* oocytes ($EC_{50} \sim 46$ μM). In contrast, although the longer chain bischoline derivatives ($n \geq 6$) bind to the *Torpedo* nAChR with similar equilibrium affinity to ACh, they have 10–50-fold higher potency in functional studies. A simple explanation for the higher potency of these longer bisquatemary ligands is that additional binding energy can be obtained from their ability to simultaneously occupy pairs of binding sites. Quantitative analysis of such a model is complicated by the changing conformational/affinity states of the receptor upon agonist exposure. While it is tempting to implicate the well-characterized sites (sites A) for ACh in both the ''crosslinking'' event and its functional consequences, there are a number of confounding issues. Numerous studies have shown that these sites do not have intrinsically high affinity in the resting state of the receptor, rather they reach their high affinity state only seconds to minutes after formation of the initial complex (reviewed in Ref. [33]). Thus, the measured affinity of the equilibrium complex cannot readily be equated with the concentration dependencies of responses that occur under pre-equilibrium conditions. A more fundamental problem in relating occupancy of sites A with receptor activation is that we have shown that their prior saturation with agonist does not inhibit channel activation upon subsequent exposure to higher agonist concentrations [34]. Thus, these sites A cannot be directly involved in either channel activation or receptor desensitization. Based on circumstantial evidence, i.e., an approximate correspondence between the estimated affinities of site B and the measured concentration dependences of both activation and desensitization, we tentatively suggested that occupancy of site B may play a role in desensitization processes [34], although there was no clear evidence for direct involvement in channel activation.

In a recent study, we identified a residue in the *Torpedo* receptor that may be involved in formation of the secondary subsite for SbCh and possibly other bisquaternary ligands [17]. Mutation of tryptophan-86 of the α-subunit (homologous to W82 of the AChBP shown in Fig. 2) to a phenylalanine had a large deleterious effect on the EC_{50} for activation by SbCh (approximately 200-fold) but only a minimal effect on the concentration dependence of ACh activation. Photoaffinity labeling studies had previously implicated this residue as a site for recognition of cholinergic ligands [35], but based on the AChBP crystal structure [12], this residue was later predicted to lie approximately 18 Å from residues that are clustered to form the high affinity binding site [6]. These results are consistent with the present study that suggests the presence of binding domains that are separated by approximately this distance.

The above discussion has thus far considered only subsites A and B in receptor responses. However, we had previously provided evidence for the existence of distinct low affinity sites on the nAChR (see [36]). These sites were revealed by monitoring of agonist-induced fluorescence changes of probe, IANBD, that had been covalently incorporated into the receptor protein. Excellent correlation between the concentration dependence of low affinity binding revealed by this fluorophore and the concentrations of agonist-induced flux responses suggested that these sites are important for channel activation. Taken together with the present data, we suggest that multiple agonist binding sites exist and that there is a dynamic interplay between binding to these sites and the observed responses. At the neuromuscular junction, the high concentrations of evoked ACh release suggest that all available binding sites will be rapidly occupied in the early stages of synaptic transmission.

In comparison to ACh, all of the bisonium compounds studied here were, at best, partial agonists of the *Torpedo*

nAChR. In some cases, such as the effects of succinylcholine or long chain analogues ($n > 8$) on the recombinant receptor, the responses were too small to be accurately quantified. There are many possible reasons to explain the reduced efficacy exhibited by some potent agonists, including formation of non-functional receptor–agonist complexes, a reduced ability of some ligands to induce the conformational changes that lead to channel opening and a decreased ion conductance through the channel. We are currently investigating these possibilities using single channel techniques to study the properties of native *Torpedo* nAChRs reconstituted in ''giant'' liposomes (see, e.g. [37]). It is becoming increasingly clear that the receptor determinants for ligand recognition are likely to be diverse and that specific interactions of structurally disparate ligands with different subsets of amino acids may dictate agonist/antagonist activity [38]. Subtle differences in receptor structure, e.g. between the *Electrophorus* and *Torpedo* receptors (see above) may also play significant roles in dictating the functional consequences of ligand binding.

In conclusion, we have studied the interaction of bisquaternary ligands with the native and recombinant *Torpedo* nicotinic receptor. Longer chain agonists, such as suberyldicholine ($n = 6$) bind with high affinity to this receptor and are also the most potent in functional studies. However, none of the bisonium compounds examined were more efficacious than the natural ligand, ACh. We suggest that the ability of some bis-quaternary compounds to crosslink pairs of subsites within the nAChR is important for their binding and functional properties.

Acknowledgments

We thank Mark W. Arriola (University of Minnesota) and Matthew A. Kula (University of Alberta) for synthesizing some of the bischoline esters used in these studies. We are grateful to Dr. Ankur Kapur who carried out preliminary studies using the recombinant *Torpedo* receptor. This work was supported by the Canadian Institutes of Health Research (SMJD and WFD), NIDA Program Project Grant DA08131 (MAR) and by a Heart and Stroke Foundation Grant (PAS). CRJC was supported by a 75th Anniversary Award, Faculty of Medicine and Dentistry, University of Alberta.

REFERENCES

[1] Raftery MA, Hunkapiller MW, Strader CD, Hood LE. Acetylcholine receptor: complex of homologous subunits. Science 1980;208:1454–6.
[2] Noda M, Takahashi H, Tanabe T, Toyosato M, Kikyotani S, Furutani Y, et al. Structural homology of *Torpedo californica* acetylcholine receptor subunits. Nature 1983;302:528–32.
[3] Unwin N. Refined structure of the nicotinic acetylcholine receptor at a 4 Å resolution. J Mol Biol 2005;346:967–89.
[4] Corringer PJ, Le-Novere N, Changeux J-P. Nicotinic receptors at the amino acid level. Ann Rev Pharmacol Toxicol 2000;40:431–58.
[5] Arias HR. Localization of agonist and competitive antagonist binding sites on nicotinic acetylcholine receptors. Neurochem Int 2000;36:595–645.
[6] Karlin A. Emerging structure of the nicotinic acetylcholine receptors. Nat Neurosci 2002;3:102–14.
[7] Prince RJ, Sine SM. Epibatidine binds with unique site and state selectivity to muscle nicotinic receptors. J Biol Chem 1998;273:7843–9.
[8] Blount P, Merlie JP. Molecular basis of the two nonequivalent ligand binding sites of the muscle nicotinic acetylcholine receptor. Neuron 1989;3:349–57.
[9] Pedersen SE, Cohen JB. D-Tubocurarine binding sites are located at alpha–gamma and alpha–delta subunit interfaces of the nicotinic acetylcholine receptor. Proc Natl Acad Sci USA 1990;87:2785–9.
[10] Hann RM, Pagan OR, Eterovic VA. The α-conotoxins GI and MI distinguish between the nicotinic acetylcholine receptor agonist sites while SI does not. Biochemistry 1994;33:14059–63.
[11] Sine SM, Kreienkamp HJ, Bren N, Maeda R, Taylor P. Molecular dissection of subunit interfaces in the acetylcholine receptor: identification of determinants of α-conotoxin MI selectivity. Neuron 1995;15:205–11.
[12] Brejc K, Dijk WJV, Klaassen RV, Schuurmans M, Oost JVD, Smit AB, et al. Crystal structure of an ACh-binding protein reveals ligand-binding domain of nicotinic receptors. Nature 2001;411:269–76.
[13] Paton WDM, Zaimis EJ. The methonium compounds. Pharmacol Rev 1952;4:219–53.
[14] Michaelson MJ, Zeimal EV. Acetylcholine: an approach to the molecular mechanisms of action. Oxford: Pergamon Press; 1973.
[15] Dunn SMJ, Raftery MA. Agonist binding to *Torpedo* acetylcholine receptor. 1. Complexities revealed by dissociation kinetics. Biochemistry 1997;36:3846–53.
[16] Dunn SMJ, Raftery MA. Agonist binding to *Torpedo* acetylcholine receptor. 2. Complexities revealed by association kinetics. Biochemistry 1997;36:3854–63.
[17] Kapur A, Davies M, Dryden WF, Dunn SMJ. Tryptophan-86 of the alpha subunit in the *Torpedo* nicotinic acetylcholine receptor is important for channel activation by the bisquaternary ligand suberyldicholine. Biochemistry 2006;45:10337–43.
[18] Elliott J, Blanchard SG, Wu W, Miller J, Strader CD, Hartig P, et al. Purification of *Torpedo* californica post-synaptic membranes and fractionation of their constituent proteins. Biochem J 1980;185:667–77.
[19] Schmidt J, Raftery MA. A simple assay for the study of solubilized acetylcholine receptors. Anal Biochem 1973;52:349–54.
[20] Neubig RR, Krodel EK, Boyd ND, Cohen JB. Acetylcholine and local anesthetic binding to *Torpedo* nicotinic postsynaptic membranes after removal of nonreceptor peptides. Proc Natl Acad Sci USA 1979;76:690–4.
[21] Elliott J, Dunn SMJ, Blanchard SG, Raftery MA. Specific binding of perhydrohistrionicotoxin to *Torpedo* acetylcholine receptor. Proc Natl Acad Sci USA 1979;76:2576–9.
[22] Moore H-P, Raftery MA. Direct spectroscopic studies of cation translocation by *Torpedo* acetylcholine receptor on a time scale of physiological relevance. Proc Natl Acad Sci USA 1980;77:4509–13.
[23] Kawai H, Carlson BJ, Okita DK, Raftery MA. Eserine and other tertiary amine interactions with *Torpedo* acetylcholine receptor postsynaptic membrane vesicles. Biochemistry 1999;38:134–41.
[24] Goldin AL, Sumikawa K. Preparation of RNA for injection into *Xenopus* oocytes. Meth Enzymol 1992;207:279–97.
[25] Barnard EA, Miledi R, Sumikawa K. Translation of exogenous messenger RNA coding for nicotinic acetylcholine receptors produces functional receptors in *Xenopus* oocytes. Proc R Soc Lond B 1982;215:241–6.

[26] Miledi R. Intracellular calcium and the desensitization of acetylcholine receptors. Proc R Soc Lond B 1980;209:447–52.
[27] Cheng Y, Prusoff WH. Relationship between the inhibition constant (K_I) and the concentration of inhibitor which causes 50% inhibition (IC_{50}) of an enzymatic reaction. Biochem Pharmacol 1973;22:3099–108.
[28] Bode J, Moody T, Schimerlik M, Raftery MA. Uses of fluorescent cholinergic analogues to study binding sites for cholinergic ligands in *Torpedo californica* acetylcholine receptor. Biochemistry 1979;18:1855–61.
[29] Wassermann NH, Erlanger BF. Agents related to a potent activator of the acetylcholine receptor of *Electrophorus electricus*. Chem Biol Interact 1981;36:251–8.
[30] Nerbonne JM, Sheridan RE, Chabala LD, Lester HA. *Cis*-3,3′-bis-{alpha-(trimethylammonium)methyl}azobenzene (*cis*-Bis-Q). Purification and properties at acetylcholine receptors of *Electrophorus* electroplaques. Mol Pharmacol 1983;23:344–9.
[31] Delcour AH, Hess GP. Chemical kinetic measurements of the effect of *trans*- and *cis*-3,3′-bis{(trimethylammonio)methyl}azobenzene bromide on acetylcholine receptor mediated ion translocation in *Electrophorus electricus* and *Torpedo californica*. Biochemistry 1986;25:1793–8.
[32] Lester HA, Krouse ME, Nass MN, Wassermann NH, Erlanger BF. A covalently bound photoisomerizable agonist. Comparison with reversibly bound agonists at *Electrophorus* electroplaques. J Gen Physiol 1980;75:207–32.
[33] McLane KE, Dunn SMJ, Manfredi AA, Conti-Tronconi BM, Raftery MA. The nicotinic acetylcholine receptor as a model for a superfamily of ligand-gated ion channel proteins. In: Carey PR, editor. Protein engineering and design. San Diego: Academic Press Inc.; 1996. p. 289–352.
[34] Dunn SMJ, Raftery MA. The role of agonist binding sites in nicotinic acetylcholine receptor function. Biochem Biophys Res Commun 2000;279:358–62.
[35] Galzi J-L, Revah F, Black D, Goeldner M, Hirth C, Changeux J-P. Identification of a novel amino acid alpha-tyrosine 93 within the cholinergic ligands-binding sites of the acetylcholine receptor by photoaffinity labelling. Additional evidence for a three-loop model of the cholinergic ligands-binding sites. J Biol Chem 1990;265:10430–7.
[36] Dunn SMJ, Raftery MA. Cholinergic binding sites on the pentameric nicotinic acetylcholine receptor from *Torpedo californica*. Biochemistry 1993;32:8608–15.
[37] Kula MA, Dunn SMJ, Dryden WF. Channel open durations in single nicotinic acetylcholine receptors are determined by ligand properties and concentration. Soc Neurosci Abs 2004;24:20.
[38] Hansen SB, Sulzenbacher G, Huxford T, Marchot P, Taylor P, Bourne Y. Structures of Aplysia AChBP complexes with nicotinic agonists and anatagonists reveal distinctive binding interfaces and conformations. EMBO J 2005;24:3635–46.